crystals

MDPI

Article

Mechanical Characterization and Microstructural Analysis of Hybrid Composites (LM5/ZrO_2/Gr)

Sunder Jebarose Juliyana [1], Jayavelu Udaya Prakash [1], Sachin Salunkhe [1,*], Hussein Mohamed Abdelmoneam Hussein [2,3] and Sharad Ramdas Gawade [4]

[1] Department of Mechanical Engineering, Vel Tech Rangarajan Dr. Sagunthala R&D Institute of Science and Technology, Chennai 600062, India
[2] Mechanical Engineering Department, Faculty of Engineering and Technology, Future University in Egypt, New Cairo 11835, Egypt
[3] Mechanical Engineering Department, Faculty of Engineering, Helwan University, Cairo 11732, Egypt
[4] Sharadchandra Pawar, College of Engineering and Technology, Someshwar, Baramati 412306, India
* Correspondence: drsalunkhesachin@veltech.edu.in

Abstract: Hybrid composites recently developed as highly effective, high-strength structural materials that are increasingly used. Aluminum matrix hybrid composites strengthened with ceramic particulates are commonly used in marine, aerospace, and defense applications because of their exceptional properties. Zirconia-reinforced composites are favored because these composites display high refractory properties, excellent abrasion resistance, and chemical resistance compared to composites of other reinforcements.For applications where lightweight and superior performance is paramount, such as parts for spacecraft, fighter aircraft, and racecars, graphite compositesare the material of choice. In this research work, an effort was made to combine the properties of zirconia and graphite by producing a unique metal matrix composite of LM5 aluminum alloy reinforced with 6% zirconium dioxide (zirconia), using the stir casting process by changing the percentage of the weight of graphite to 2%, 3%, and 4%. The test specimens were prepared and evaluated in compliance with ASTM standards to study micro- and macrohardness, and impact, tensile, and compressive strength. Microstructural studies of composites performed through optical microscopy and SEM expose the unvarying dispersal of particulates of ZrO_2/graphite in the aluminum matrix. The hardness, impact, and compressive strength are enhanced due to the addition of reinforcement.

Keywords: hybrid composites; characterization; zirconia; graphite; SEM; microstructure

check for updates

Citation: Juliyana, S.J.; Prakash, J.U.; Salunkhe, S.; Hussein, H.M.A.; Gawade, S.R. Mechanical Characterization and Microstructural Analysis of Hybrid Composites (LM5/ZrO_2/Gr). *Crystals* **2022**, *12*, 1207. https://doi.org/10.3390/cryst12091207

Academic Editors: Yang Zhang and Yuqiang Chen

Received: 30 July 2022
Accepted: 22 August 2022
Published: 27 August 2022

Publisher's Note: MDPI stays neutral with regard to jurisdictional claims in published maps and institutional affiliations.

Copyright: © 2022 by the authors. Licensee MDPI, Basel, Switzerland. This article is an open access article distributed under the terms and conditions of the Creative Commons Attribution (CC BY) license (https://creativecommons.org/licenses/by/4.0/).

1. Introduction

Aluminiummatrix composites (AMCs) are recognized as materials with enhanced reliability for specific engineering fields. In some instances, they substitute homogenous alloy systems and, in particular cases, similar materials in terms of efficiency and economy [1,2]. Among several light metals such as Mg, Al, and Ti used as matrices, Al and its alloys are used more extensively as the matrices for MMCs [3,4]. This is related to properties such as being lightweight, and having a high corrosion resistance and ease of fabrication, which satisfy a broad range of current and potential requirements [5,6]. LM5 is a widelyused choice of special-purpose alloy as a matrix material compared to several other types of aluminium alloys, due to its favorable mechanical properties combined with efficient formability and corrosion resistance used for marine applications. Aluminium alloys have a meager resistance to wear compared with other metallic materials. To increase toughness and strength, the aluminium alloy must be reinforced. A variety of materials such as silicon carbide (SiC), titanium carbide (TiC), boron carbide (B_4C), aluminium oxide (Al_2O_3), silicon nitride (Si_3N_4), zirconium dioxide (ZrO_2), zirconium silicate ($ZrSiO_4$), boron nitride (BN), and sometimes even softer materials such as graphite and mica,are also used as reinforcements. The materials that stand outare ceramics rather than ferrous

alloys. A good composite can be fabricated with ceramic reinforcement, and it exhibits superior qualities that are comparable to, or even greater than, other ferrous alloys. The liquid metallurgy techniques are easier to tackle during manufacturing and have a low-cost manufacturing method, particularly with intermittent reinforcements, compared to various processing techniques. It is observed that these MMCs result in isotropic properties [7]. A decent number of studies were conducted individually on Al/ZrO_2 and Al/graphite. The effect of graphite on the mechanical properties of aluminium composites was explored by Pai et al. [8].

The use of multiple reinforcements improved tribological properties for aluminum matrix hybrid composites more than the use of a single reinforcement. The constituents can interact synergistically, giving rise to better properties. Aluminium matrix composites with zirconia (ZrO_2) reinforcementswith high fracture toughness were produced by squeeze casting to fabricate Al-9Zn-6Mg-3Si composites with additions of 2.5, 5, and 7.5 vol.% ZrO_2. The results reveal that the higher the porosity, the higher the hardness, and the higher the impact values, both in the as-cast condition and after 1 h of ageing at 200 °C [9]. Aluminium metal matrix replaces traditional materials with high melting points and high densities, reducing energy consumption and helping the environment. With the help of AA 6061 and ZrO_2, they produced a low-weight, high-strength composite material using a stir casting technique combined with a squeeze casting configuration [10].The mechanical properties are enhanced, and there is a slight increase in density due to the high density of ZrO_2, up to the addition of 6% ZrO_2 [11].

The compo-casting technique successfully creates aluminium Al7075 alloy composites with varied weight percentages of ZrO_2 reinforcement (3, 6, 9, 12). The micrographs and EDAX show a homogeneous reinforcement distribution in a soft aluminium-rich matrix with micro porosities. The test findings show that the composites' hardness and ultimate tensile strength are increasing up to a reinforcement percentage of 6%, and there is a significant improvement in characteristics, but after that, the improvement is small. The gains in characteristics are mostly attributable to greater reinforcement distribution and interfacial bonding [12]. The mechanical and tribologicalbehaviour of aluminium (Al)-based silicon carbide (SiC, micro particles) and zirconium-oxide (ZrO_2, nano particles)-particle-reinforced hybrid composites. Powder metallurgy (PM) technology was used to add ZrO_2 (0, 3%, 6%, and 9%, weight fraction) to Al-5% SiC composites. The hardness and wear resistance of Al + SiC + ZrO_2 hybrid composites are shown to improve as the ZrO_2 content is increased [13].

Metal matrix composites based on aluminium alloys are becoming more popular in industrial applications that demand a high strength-to-weight ratio. AA6061 aluminium alloy matrices with zirconium-dioxide-particle-reinforced composites were fabricated using the stir casting technique.Composite materials reinforced with zirconium dioxide are fabricated with various weight percentages of reinforcement, such as 2%, 4%, 6%, 8%, and 10%. The composite's metallurgical and mechanical properties are investigated. The particles are equally spread in the matrix alloy, as shown by a scanning electron micrograph. The addition of ceramic particles increases the material's hardness by preventing dislocations in the alloy matrix. The addition of zirconium dioxide particles boosts its strength by 6%, according to tensile test results. In 6% of ZrO_2 and 2% of C inclusion of a 92% of AA6061 matrix material, the maximum strengths are 175 MPa in tensile strength, 45HRB hardness, and 4.56×10^{-9} g/mm. The addition of ZrO_2 raises the hardness of the base metal from 6% to 12%, and increases the ultimate tensile strength from 8% to 15%. The characteristics of the composite material are lowered when the reinforcing particles are added to the highest extent possible [14].

Al 2024 composites reinforced with 5%, 10%, 15%, and 20% ZrO_2 are created via vacuum infiltration. Due to an increase in the ZrO_2 reinforcement ratio, the density steadily rises. The density increase is due to the density of the reinforcing element being greater than the density of the matrix material. The rise in density, on the other hand, is not as great as the increase in the ZrO_2 reinforcement ratio. Reinforcement agglomeration in the composite

structure is generated by increasing the ZrO_2 reinforcement ratio. In general, graphite as an additive to a composite has an eclectic effect on mechanical properties, whereas it leads to a positive effect on tribological properties [15]. Graphite is accessible in large quantities and at a lower cost. It is used to minimize the energy content, material content, cost, component weight, and improve wear resistance in aluminium castings. Strong interfacial connections exist between the matrix and the graphite particles. Hardness reduces as graphite content rises, but wear characteristics improve [16].

AA7075/graphite composites were produced by the stir casting method. The weight % of the graphite reinforcement in the AA7075 matrix phase varies from 5 to 20% in steps of 5%. A decrease in the ultimate tensile strength of the composite compared to the base matrix with an increase in the addition of graphite in the composite is observed. A significant decrease in the tensile strength is noticed at 5% of graphite compared to other weight percentages of graphite. This is due to graphite, which is brittle in nature, augmenting the tendency of crack initiation and propagation at the metal interface [17].

The tensile test results of Al 6061/B_4C/graphite with a constant weight percentage of B_4C and varying weigh percentage of graphite are demonstrated. There is an increase in the tensile strength of composite with the addition of B_4C, whereas a decrease in the tensile strength with the addition of graphite is noticed. They conclude that the tensile strength of MMC mainly depends on reinforcement strength and interfacial strength between the matrix and the reinforcement. ZrO_2 was added to the aluminium 2% graphite matrix in four distinct amounts (3%, 6%, 9%, and 12%). Cold pressing with a pressure of 700 MPa produces green compact samples from composite powders that were mechanically alloyed for 60 min. The green compacts were sintered at 600 °C for 2 h. Microstructure, density, and hardness measurements were taken on the aluminium composites formed. Hardness and density values increase as the amount of ZrO_2 increases in the matrix, and decrease as graphite is added as a consequence of the research [18].

The inclusion of graphite to the Al6061 matrix demonstrates a worsening trend in mechanical properties. The influence of SiC and graphite on Al6061 alloy is demonstrated by the fact that the composite's hardness and strength increase with the addition of SiC, while the hardness decreases and the strength increases with the inclusion of graphite to Al6061.

Aluminum alloys have excellent mechanical properties. Zirconium dioxide improves strength, rigidity, and resistance to temperature, with a slight increase in composite density. Graphite decreases density and enhances wear properties. Particulates are readily available, and processing is easy, while fabrication costs are low. Stir casting is the optimal and economical processing route for AMCs. In particular, magnesium improves aluminum/zirconium dioxide andgraphite wettability.

Very few works were identified in analyzing the effect of ZrO_2 on mechanical and metallurgical properties [19–21]. No work was identified in analyzing the effect of ZrO_2 and graphite on LM5 base material while subjected to mechanical and metallurgical properties [12]. Hence, this work mainly concentrated on developing new composite material by taking LM5 as the base material with 6% ZrO_2, and by varying the weight percentage of graphite to 2, 3, and 4% to identify the effect of ZrO_2 and graphite on the mechanical and metallurgical properties.

2. Materials

2.1. Matrix Metal

Aluminum alloy LM5 was the matrix material. The alloy is used where very high corrosion resistance from seawater or marine atmospheres is needed, for equipment used in the manufacture of foodstuffs, cooking utensils, and chemical plants, and the casting of highly polished surfaces. Accordingly, they are famous for decorative casts and casts used in dairy and food handling equipment, marine and chemical pipe fittings, and architectural/ornamental marine hardware applications. LM5's chemical composition

was examined using optical emission spectrometry as per ASTM E 1251-07 standard, presented in Table 1.

Table 1. Chemical composition of LM5 aluminum alloy.

Cu	Mg	Si	Mn	Fe	Pb	Zn	Al
0.032	3.299	0.212	0.022	0.268	0.02	0.01	Balance

2.2. Reinforcement

Zirconium dioxide (ZrO_2), the crystalline oxide of zirconium, also called zirconia, is a widely studied ceramic element. Zirconia (ZrO_2) was chosen as the reinforcement particle because of its easy accessibility and suitability for high-temperature applications. Producing zirconia comprises the collection and elimination of unnecessary ingredients and impurities. Extraction of zirconia has many routes, including plasma disassociation, chlorine and alkali oxide decomposition, and lime fusion. Similar to other ceramic materials, zirconium oxide is a substrate with a high tolerance to the propagation of cracks. Therefore, zirconium oxide ceramics are often thermally developed; they are also the material of choice for joining ceramics and steel. Very low thermal conductivity and high strength are a desirable combinations of properties [22–24].

2.3. Fabrication of LM5/ZrO_2/Gr Hybrid Composites

The stir casting assembly had a C-Type closed furnace with a capacity of 5KVA (optimal temperature ranges from 500 °C to 1100 °C), with a stirrer assembly (Remi RQM-122/R) utilized to fabricate the composite. The stirrer had a stirring shaft of 350 mm length and 6 mm diameter made of SS304, and had a chuck for easy interchangeability of the shaft. It had a pitched fan type impeller of diameter 38 mm with 4 blades. The impeller was made of high chromium steel with high carbon content coated with zirconia, and was mounted on a vertical variable-speed motor with a range between 20 and 1500 rpm. The silicon carbide crucible was kept within the furnace. Figure 1a shows the stir casting set-up used for this research work, Figure 1b shows the pouring of the molten mixture into the mold, and Figure 1c shows the fabricated composite specimen.

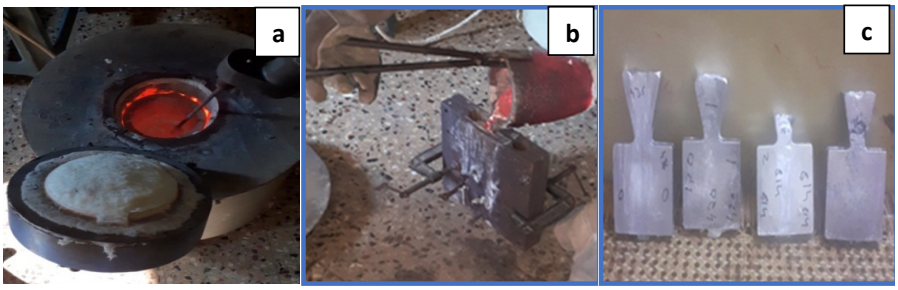


Figure 1. (**a**) Stir casting set-up; (**b**) pouring into die; (**c**) composite specimen.

Initially, the LM5 alloy, as tiny ingots, was charged and heated to about 850 °C in the silicon carbide crucible until the whole alloy was melted in the crucible. Zirconium dioxide and graphite particles were preheated for 20 min to 200 °C in a muffle furnace of 4 KVA, to eliminate the moisture existing in the reinforcement. A vortex was created in the molten metal by the stirrer, which was slowly lowered into the melt. Then, the preheated ZrO_2 of average particles size 70 µm and graphite of 30 µm were slowly mixed into the liquid metal at a steady rate, by maintaining the stirring speed at 600 rpm [25,26]. Magnesium powder 0.5% is added as a wetting agent to enhance the proper mixing of the matrix and the reinforcement [27]. The stirring continued for 7 min even after particle feeding was completed. Hexafluoro ethane tablets were introduced into the mixture before pouring into the mold to minimize the porosity. The temperature for pouring was kept at 750 °C. To achieve uniform solidification, before pouring the mixture into the mold, the

mold was also preheated to 650 °C. This process was used to manufacture three sets of novel hybrid composites made of special-purpose aluminum alloy LM5 reinforced with 6% ZrO_2 particles and graphite 2, 3, and 4%. The melt was poured into the preheated mold to fabricate the hybrid composites.

3. Testing of AMCs

3.1. Micro Structural Analysis

3.1.1. Optical Microscopy

An inverted optical microscope was used to examine the MMCs. Abrasive papers were used to make the surfaces of the specimen smooth, and then it was polished through 220 to 1500 mesh with velvet fabric. Before microscopic analysis, the specimens were then etched using HF solution. Metallographic assessments offer strong quality assurance and a practical analysis resource. The specimens obtained from each composite were precisely polished to match the texture of the surface. Figure 2 shows the specimens used for the microstructure analysis.



Figure 2. Composite specimens for microstructural analysis.

The role of a microstructure on a material's physical and mechanical properties is influenced by the numerous flaws that exist or are absent in the structure [28]. These flaws can come in many forms, but the main ones are the pores. These pores play a decisive role in finalizing the characteristics of materials and their formulation. Moreover, for some materials, there can be various phases at the same time. These phases may have various properties, and prevent the material from fracturing if treated correctly.

3.1.2. SEM and EDAX

The crystal structure of materials is a 'fingerprint' of processing. A composite's microstructure is studied to recognize the changes in the structure of the parent metal after the addition of a reinforcement [29,30]. SEM has many advantages such as simple preparation of the specimens, broadest possible magnification scale (commonly between 15 and 50,000 times), and the capacity to observe large regions of the surface of the specimen, including the origin and spread zones. The surface can indeed be placed straight into the microscope, which has excellent field depth for concentrating on largetopographical surfaces.

EDAX is an analytical tool for using a sample's elemental analysis or chemical composition. It focuses on the interactions of a sample by supplying X-ray excitation. The characterization capabilities are primarily due to the underlying theory where each element has a unique atomic structure that causes its electromagnetic emission spectrum to have a unique set of peaks, which is the main principle of spectroscopy. A pulse of X-ray is centered on the examined material to induce the release of characteristic X-rays from a specimen. At resting, an atom inside the sample contains electrons at different energy levels, or electron shells attached to the nucleus in the ground state or unexcited. An energy-dispersive spectrometer can determine the amount and energy of X-rays released from a specimen. Since the X-ray energies indicate the energy difference between the two shells and the emitting element's atomic structure, EDAX makes it possible to measure the elemental composition of the specimen.

3.2. Density

Density is the naturally occurring phenomenon that reveals the characteristics of the composite. Utilizing displacement procedures, the density of a composite is calculated quantitatively, using an electronic weighing machine with a density calculating kit as per the ASTM: D 792-66 test procedure. Theoretical density is the actual density of a material corresponding to the limit that products with total density can achieve without pores. Many materials typically consist of a mixture of structural molecular components, each with their own mass. Archimedes proved very ingeniously that when an object is immersed in water (or any fluid), the force that it experiences is proportional to the mass of the water displaced times gravity (i.e., water weight). Density can be calculated using the standard formula. Porosity is the amount (or volume) of space in a material relative to the total size of the material. It is a mathematical ratio: void volume divided by total volume (vacuum/total); this ratio is usually multiplied by 100 to be compared in percentages rather than decimals [30]. It is calculated using the expression (Equation (1)).

$$\text{Porosity \%} = (\text{Theoretical Density} - \text{Experimental Density}) \times 100/\text{Theoretical Density} \quad (1)$$

3.3. Microhardness

Vickers hardness testing tool is often used to evaluate the composite's microhardness. Microhardness tests may be used to provide the data needed to measure discrete microstructures into a broader matrix, to evaluate excellent foils, or to assess a specimen's hardness gradient along a transverse. Microhardness testing refers specifically to the static indentations of 1 kgf or fewer loads. The Vickers hardness test uses a 136° apical angle diamond. The surface to be tested usually needs to be smoothly polished [31,32]. Amicroscope of 500× magnification is required to measure the shaped indents directly. Specifications of the Vickers hardness measurements are ASTM E 92 (for 1 kgf to 120 kgf) and ASTM E 384 (for force inferior to 1 kgf).

3.4. Macrohardness

Macrohardness is the measurement of the hardness of materials tested with high applied loads. The macrohardness measurement of materials is a quick and simple method of obtaining mechanical property data for the bulk material from a small sample. The Rockwell test measures the penetration depth of the indenter under a significant load (large load) in contrast to the penetration made by a minor load (preload). Here, various scales are represented by a solitary letter, which uses various indenters or loads [33–35]. An outcome is a dimensionless number given as HRA, HRB, HRC, HRE, etc., whereas the preceding letter is the Rockwell scale.

3.5. Tensile Strength

Tensile test was performed under atmospheric conditions using a computerized universal testing machine (model FMI F-100), with a cross head speed of 2 mm/min, to assess the manufactured composite materials. The specimens were prepared to ASTM-E8 standards. The findings of the tensile test are used in the selection of engineering materials. The strength of a material is always the prime concern, and can be determined by measuring the stress needed for severe plastic deformation, or the maximum stress tolerated by the material [36,37]. The material's ductility is also of concern, which measures its bend until it breaks. Tensile strength (also known as ultimate tensile strength) is quantified by dividing the maximum force held by the specimen by the initial cross-sectional area of the specimen during the stress test. Both the original gauge length and the percentage increase must be considered when recording the elongation values.

3.6. Compressive Strength

Compression testing was performed under atmospheric conditions using a computerized universal testing machine (model FMI F-100), with a cross head speed of 2 mm/min,

to assess the manufactured composite materials. The research specimens (Figure 3) were prepared to ASTM-E8 standards. The findings of the compressive test are used in the selection of engineering materials. The material requirements must provide compressive properties to ensure performance [38,39].



Figure 3. Compressive test specimens.

Compressive testing reveals how the material can react as it is squeezed. Compression testing evaluates the action or reaction of the material against crushing loads, and assesses a material's plastic flow behaviour and ductile fracture limits. A compression test is a procedure for evaluating the behaviour under a compressive load of materials. Compression experiments are carried out by loading the test sample between two parallel plates and then bringing the crossheads together, adding force to the sample [40].

3.7. Impact Strength

Impact resistance of any material is the capability of that material to withstand a force applied or a sudden load [41,42]. Usually, it is distributed as the amount of mechanical energy consumed under the impact load imposed throughout the deformation process, and is presented as energy lost per unit of J/m^3. The Izod impact test is a standard ASTM tool for determining resistance to material impacts. A swivel arm (constant energy potential) is lifted to a particular height, and afterward, it is lowered. The arm falls to a notched plate and breaks it. The energy consumed by the plate is measured by the height at which the arm swings after it hits the plate. In the Izod impact test, the sample (ASTM A-370 standards) is mounted in a cantilever beam configuration, in contrast to a three-point bending configuration. Figure 4 shows the photograph of specimens used for impact strength testing.



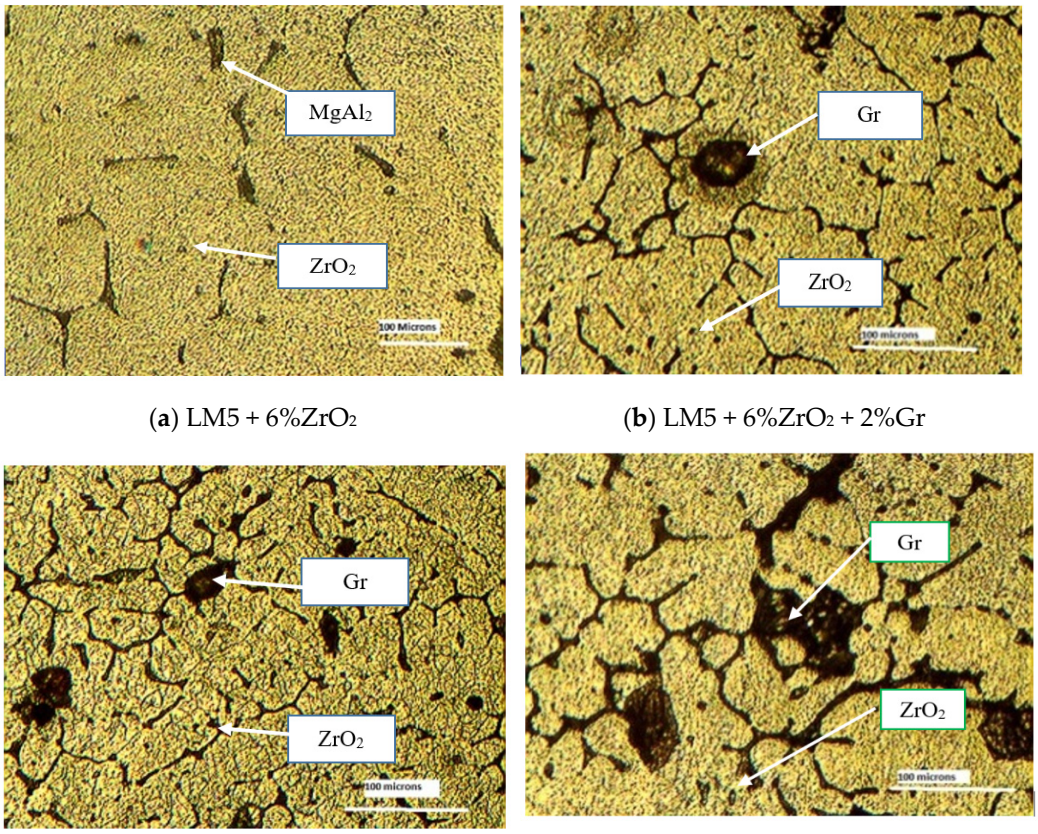
Figure 4. Impact test specimen.

4. Results and Discussions

4.1. Microstructural Analysis

4.1.1. Optical Micrograph Analysis

Microstructural analysis's primary purpose is to examine the stratified dispersal of reinforcement particles into the matrix. The optical imaging micrographs demonstrate the homogeneous spread of the zirconia and graphite particles into the matrix. When the weight percentage of the strengthening material (reinforcement) increases, the particles in the particle distribution begin coagulating and disrupting uniformity [43]. Uniform reinforcement spread provides the matrix strength; the same would be the fundamental cause for accelerated mechanical properties. Figure 5 reveals the microstructures of base metal aluminum B.S.1490 grade LM5 aluminum–magnesium alloy and LM5/ZrO_2/Gr composites at 200× magnification.



(**a**) LM5 + 6%ZrO_2 (**b**) LM5 + 6%ZrO_2 + 2%Gr

(**c**) LM5 + 6%ZrO_2 + 3%Gr (**d**) LM5 + 6%ZrO_2 + 4%Gr

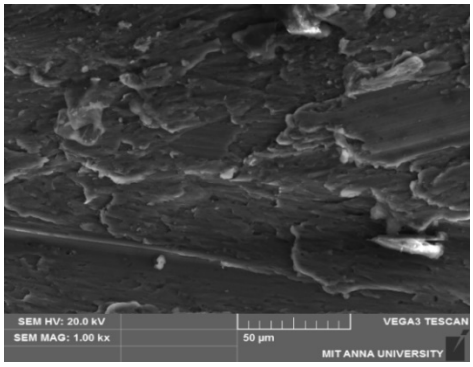
Figure 5. Micrographs of hybrid composites.

The microstructure of LM5 shows theinterdendritic pattern of primary aluminum grains. The grain boundaries are precipitated with $MgAl_2$ eutectic particles, which have not dissolved during the solidification. The primary aluminum phase grain size is measured as 40 to 50 microns. The microstructure of the hybrid metal matrix composites with 6% ZrO_2 and 2, 3, and 4% of graphite shows the distribution of particles of ZrO_2 and graphite. The particles are inside the primary aluminum grains. The micrograph shows the resolved particles of the composite particles [44,45]. However, the composite with 6% ZrO_2/Gr particles distribution is observed, and they present as clusters along the grain boundaries.

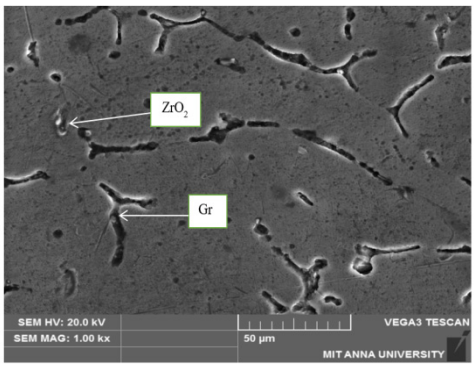
4.1.2. SEM Analysis

Figure 6 shows the SEM images of LM5 and LM5/ZrO_2/Gr composites. Scanning electron micrographs display the unvarying dispersal of ZrO_2 ceramic particles and graphite

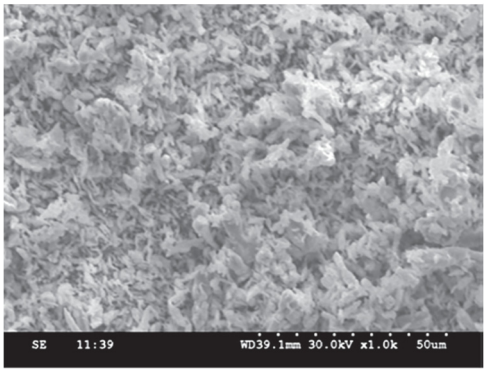
in the aluminum MMCs at lower magnifications, and the findings of the SEM display the matrix–particle interfaces at higher magnifications [46,47]. These figures reveal the relatively homogenous distributions of reinforced ZrO_2 particles and graphite with aluminum alloy. In comparison, these statistics demonstrate the uniformity of the composite materials. The properties of MMCs depend on the metal matrix, the weight percentage, the arrangement of particle reinforcement, and the binding of the interface seen among particles and the matrix. No pores are found in either case, suggesting improved wettability between the matrix and the reinforcement particles [48,49].



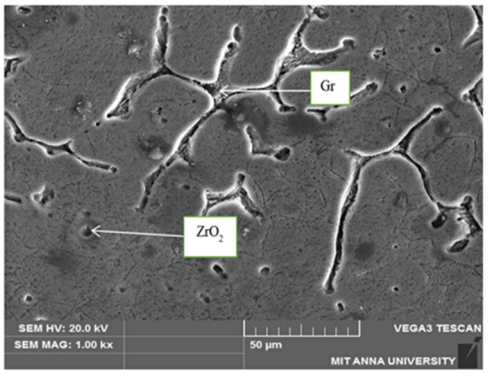
(**a**) LM5



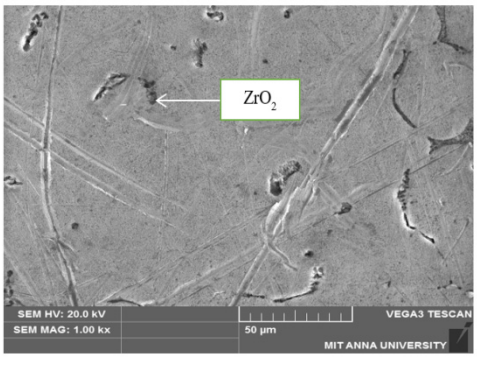
(**d**) LM5 + 6% ZrO_2 + 2%Gr



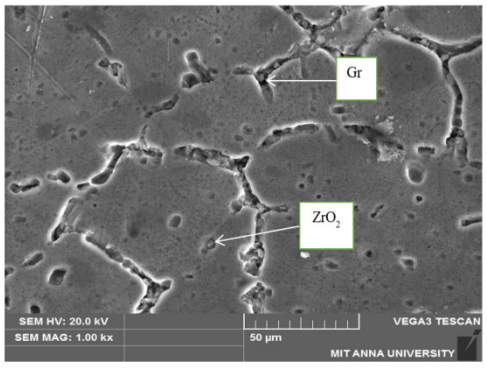
(**b**) ZrO_2



(**e**) LM5 + 6% ZrO_2 + 3%Gr



(**c**) LM5 + 6%ZrO_2



(**f**) LM5 + 6% ZrO_2 + 4%Gr

Figure 6. SEM images of hybrid composites.

The interfacial bonding is accomplished in this case due to fast cooling. It is also noticed that the area fraction rises as the weight percentage of ZrO_2 reinforcement rises, seen in the micrographs as a white field, and graphite particles are seen as a black field.

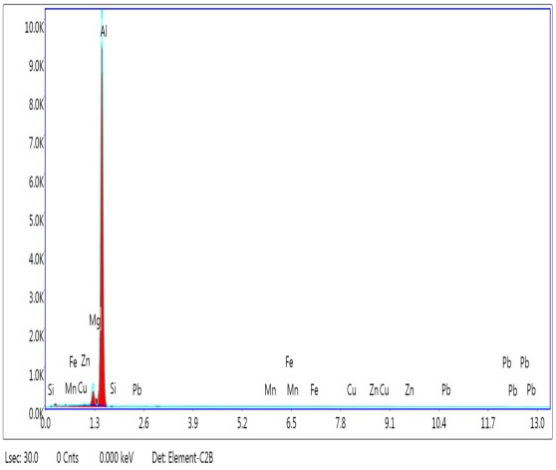
The average grain size of the aluminium LM5 matrix reduces as the ZrO_2 reinforcement weight fraction increases. It is also suspected that mechanical properties are rising due to the rise in the interfacial bonding of the reinforcements with the aluminium matrix alloy. This is due to the gravity of ZrO_2 and graphite, and is consistent with the effective selection of stirring parameters and substantial wetting of preheated ZrO_2 particles before being applied to the alloy of the matrix.

4.1.3. EDAX Analysis

EDAX develops the best solutions for micro-and nano-characterization, where primary and structural information is required, making analysis more accessible and accurate.

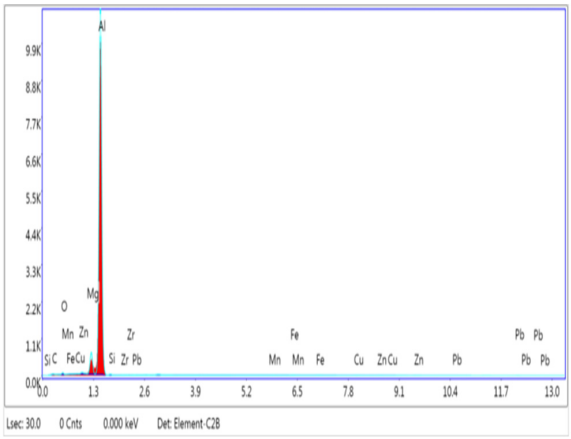
The existence of reinforcement and unit percentage of the composites is confirmed by EDAX analysis (Figure 7). EDAX demonstrates the pattern of particles of ZrO_2 and graphite particles scattered in composites of the aluminum matrix.

Element	Weight %	Atomic %	Error %
Mg	4.46	4.95	3.98
Al	93.68	93.86	2.33
Si	0.73	0.70	26.33
Pb	0.13	0.02	66.09
Mn	0.17	0.08	67.48
Fe	0.46	0.22	61.10
Cu	0.29	0.12	67.58
Zn	0.09	0.04	72.18



(**a**) LM5

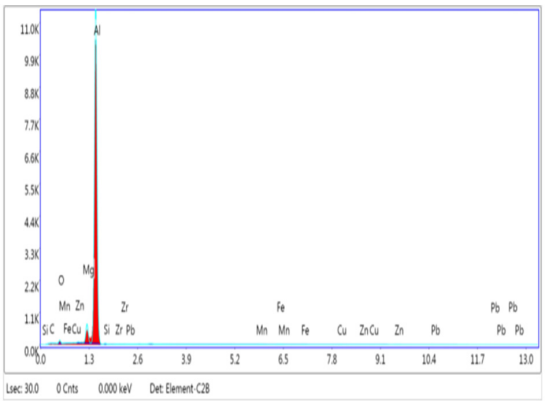
Element	Weight %	Atomic %	Error %
C	0.36	0.80	99.99
O	1.72	2.86	18.79
Mg	4.41	4.83	4.11
Al	91.92	90.67	2.40
Si	0.39	0.37	38.16
Zr	0.13	0.04	88.13
Pb	0.16	0.02	74.17
Mn	0.20	0.10	66.93
Fe	0.30	0.14	62.12
Cu	0.20	0.08	71.27
Zn	0.20	0.08	67.32



(**b**) LM5 + 6%ZrO_2 + 2%Gr

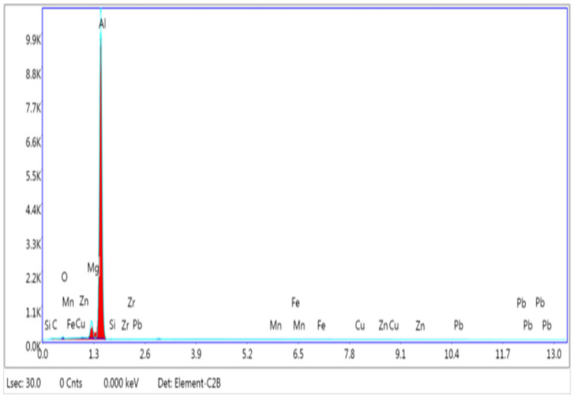
Figure 7. *Cont.*

Element	Weight %	Atomic %	Error %
C	1.75	3.83	75.93
O	1.37	2.24	25.13
Mg	4.76	5.14	4.04
Al	90.12	87.68	2.48
Si	0.64	0.60	24.16
Zr	0.19	0.06	80.08
Pb	0.18	0.02	76.76
Mn	0.18	0.09	67.98
Fe	0.32	0.15	61.44
Cu	0.23	0.10	69.36
Zn	0.26	0.10	65.44



(**c**) LM5 + 6%ZrO_2 + 3%Gr

Element	Weight %	Atomic %	Error %
C	0.84	1.83	84.68
O	2.75	4.51	17.01
Mg	4.62	4.98	4.02
Al	90.22	87.76	2.43
Si	0.59	0.55	28.17
Zr	0.22	0.06	78.72
Pb	0.10	0.01	77.12
Mn	0.17	0.08	68.08
Fe	0.22	0.10	63.90
Cu	0.19	0.08	68.23
Zn	0.09	0.04	73.91



(**d**) LM5 + 6%ZrO_2 + 4%Gr

Figure 7. EDAX images of hybrid composites.

4.2. Density

The experimental and theoretical density of the fabricated LM5/6% ZrO_2 composite is found to be 2.73 and 2.832 g/cm^3, respectively, and the density of all the graphite composites is less when compared with the density of the ZrO_2, because of graphite's low density (2.26 g/cm^3).

The porosity of the produced composites slowly increases, since eutectic alloys have a high tendency to form large pores by increasing the weight percentage of the reinforcement [50]. Figures 8 and 9 shows the effect of graphite on the density and the porosity of AMCs, respectively.

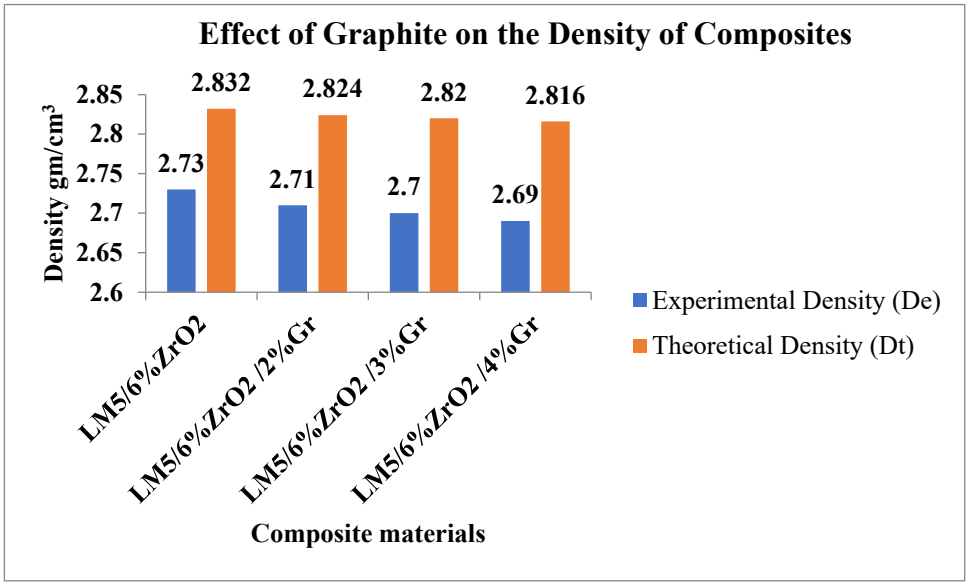


Figure 8. Effect of graphite on the density of composites.

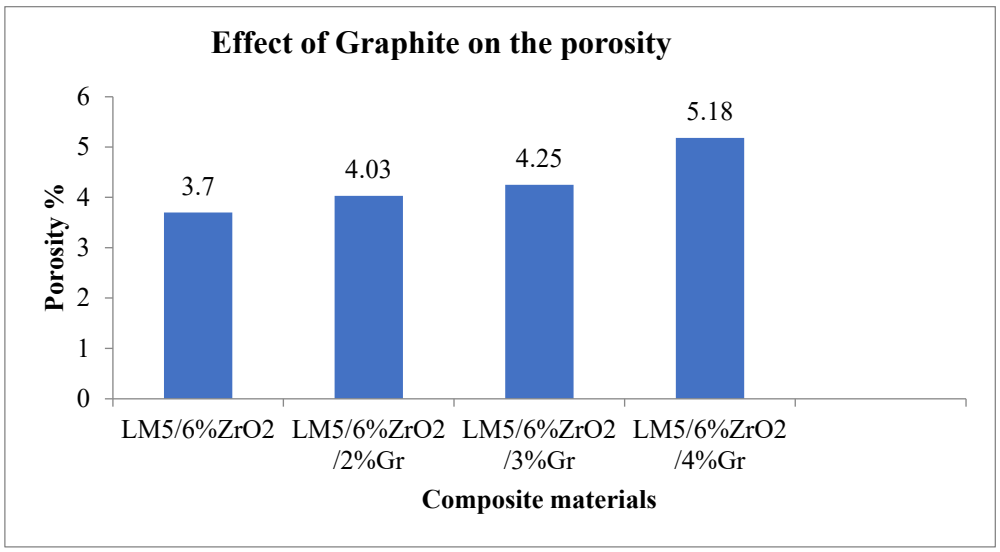


Figure 9. Effect of graphite on the porosity of composites.

4.3. Microhardness

Microhardness tests were performed at room temperature in the Vickers hardness measurement device by introducing a load of 0.5 kgf for 10 s of dwelling time. Figure 10 shows the effect of graphite on the microhardness of AMCs. The highest value is 74 VHN for the 6% ZrO_2 composite. It indicates higher hardness. The introduction of graphite into the metal matrix decreases the hardness value. From Figure 10, it can be observed that the hardness is decreased linearly with an addition of the graphite reinforcement [51,52]. When adding the graphite particles to the composites, the surface area of the reinforcements is increased, and the particle dimensions of the matrix are reduced.

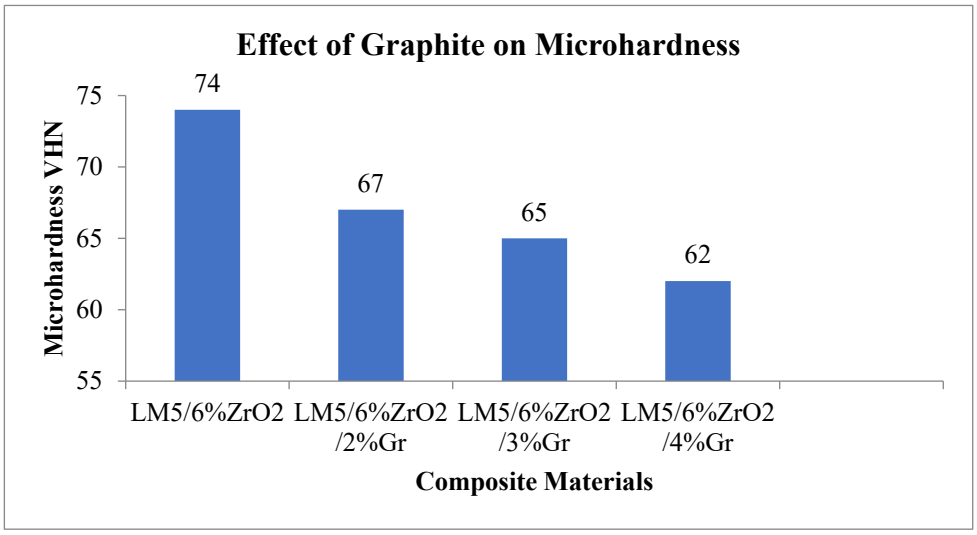


Figure 10. Effect of graphite on the microhardness of composites.

4.4. Macrohardness

The effect of graphite on the macrohardness is shown in Figure 11. The Rockwell hardness value of LM5/6% ZrO_2 alloy is 67HRE. The hardness value decreases dramatically to 60HRE, 59HRE, and 57HRE for 2, 3, and 4 graphite weight percentages, respectively. The appearance of very soft particles of graphite makes plastic distortion more opposed, contributing to decreased material hardness.

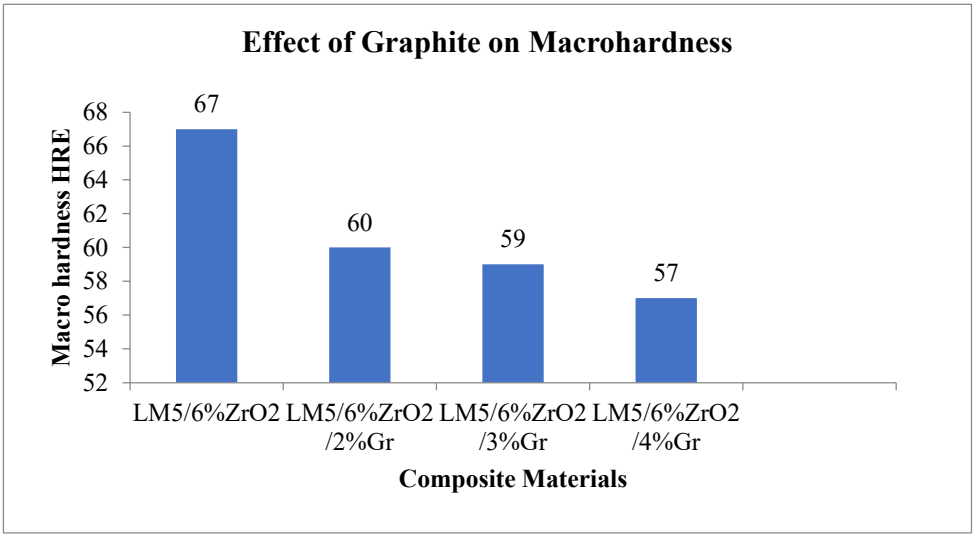


Figure 11. Effect of graphite on the macrohardness of composites.

4.5. Tensile Strength

The tensile test shows that the strength of the composites rises as the weight % of the ZrO_2 particles increases. Sample stress–strain curves of tensile test specimens are shown in Figure 12. Fractured tensile test specimens are shown in Figure 13.

Figure 14 shows the effect of zirconium dioxide and graphite weight percentage on the hybrid aluminum matrix composite's tensile strength. Zirconia has a monoclinic composition, while the composition of aluminum crystallizes in FCC. Their interface strength is due to the different crystalline structures of zirconia and aluminum that sounds incoherent [53,54].

This incoherence, therefore, increases the strength of the composite materials. The high hardness of the Al matrix composites is probably due to the high stiffness rate of the

composites during their strain. Improvement of the hardening function may be related to the elastic properties of ZrO_2 particles and their prevention of deformation of the matrix. Thus, in the presence of a suitable interface, the ZrO_2 particles prevent the deformation of the matrix and increase work hardening. In addition, the specific thermal expansion coefficients of zirconia (10×10^{-6} K^{-1}) and aluminum (16×10^{-6} K^{-1}) produce stress that can boost the number of dislocations and, as a result, the strength of the composite. Increasing dislocation density and the piling up behind ZrO_2 particles serve as obstacles in dislocation movement. The greater the sum of ZrO_2, the greater the number of dislocations that are formed [55]. The tensile strength of the reinforced composite of aluminum alloy LM5 with 6% ZrO_2 is 220 MPa, and this value decreases to 216 Mpa for LM5/6% ZrO_2/2% Gr, and decreases again to 215 MPa for the composition of LM5/6% ZrO_2/3% Gr. From the experimental results, it is clear that the tensile strength of the composites slightly decrease compared to the 6% ZrO_2, due to the addition of graphite particles.

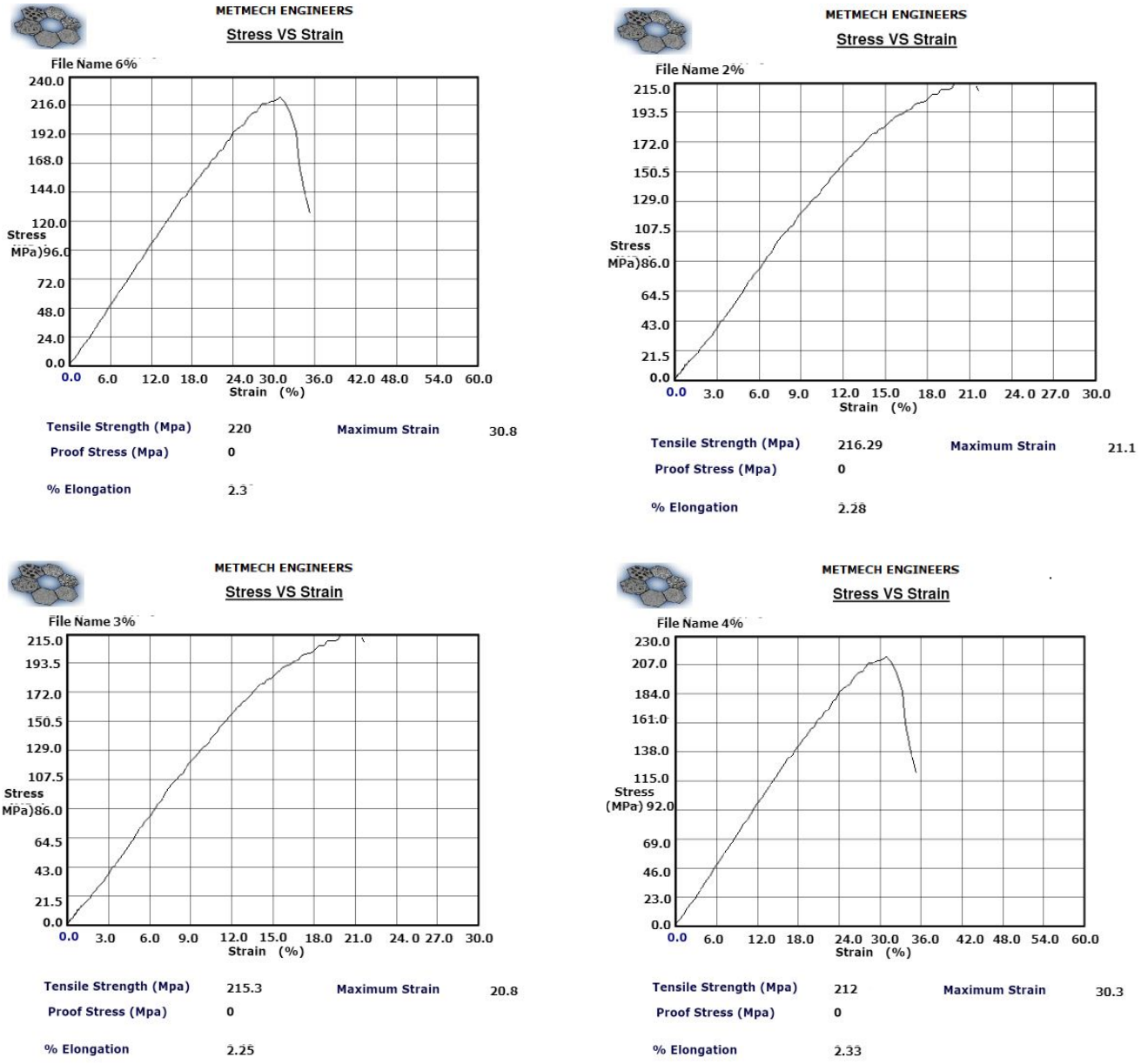


Figure 12. Sample stress–strain curves of tensile test specimens.



Figure 13. Fractured tensile test specimens.

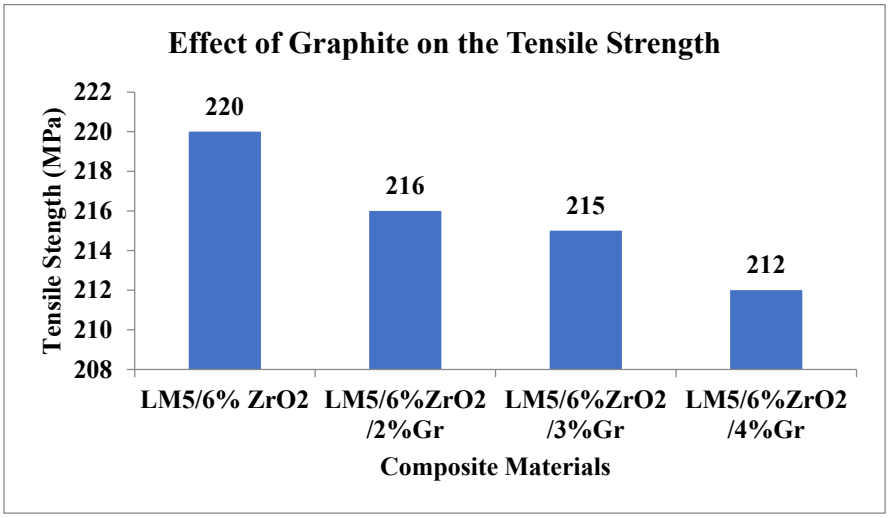


Figure 14. Effect of graphite on the tensile strength of composites.

Figure 15 shows the effect of zirconium dioxide and graphite on the elongation percentage. Results show that by adding the weight percentages of zirconium dioxide, the elongation of the material decreases. The LM5 loses its ductility, and transitions from ductile to brittle by adding the zirconium dioxide. The elongation of LM5 + 6% ZrO_2 is 2.3%; this value is reduced to 2.28%, 2.25%, and 2.23% for the graphite composites. Due to the brittleness of the fabricated composite tensile strength, elongation and strain are less for graphite composites compared to 6% ZrO_2. The maximum ultimate tensile strength is observed at 6% ZrO_2, but graphite may enhance wear properties. Few cluster creation are noticed in the 4% graphite reinforcement, which is projected to cause decreased mechanical properties, particularly tensile strength.

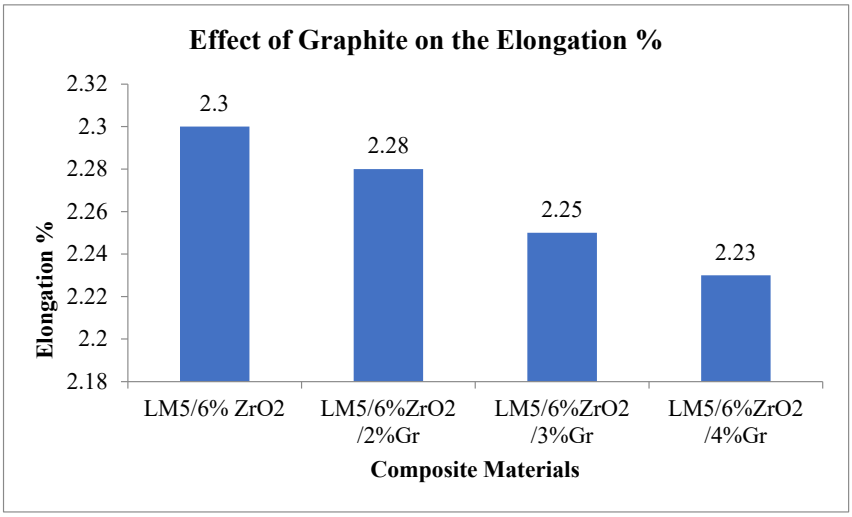


Figure 15. Effect of graphite on the elongation %.

4.6. Compressive Strength

The compressive test exposes that the strength of the LM5/6% ZrO_2/Gr composites rises as the weight % of the particles in Gr increases. Sample stress–strain curves of the compression test specimens are shown in Figure 16. Distorted compression test specimens are shown in Figure 17.

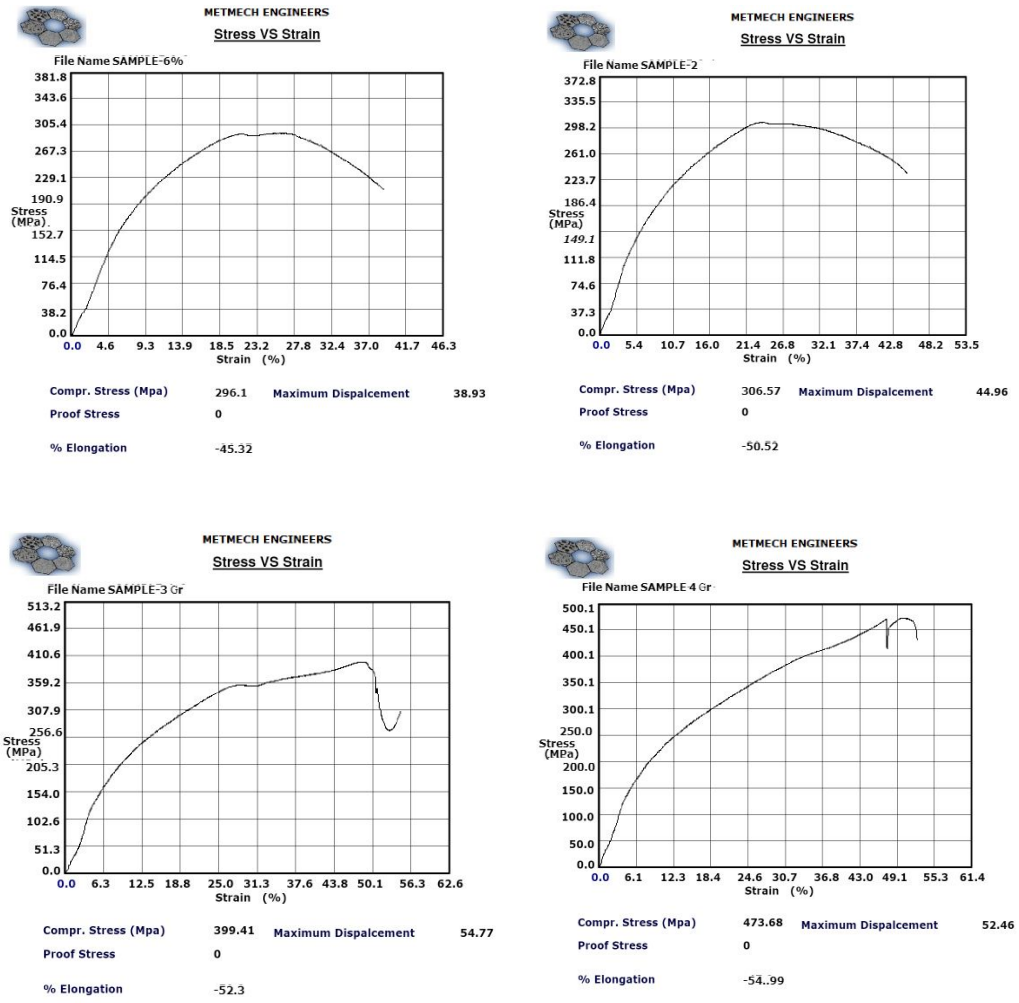


Figure 16. Sample stress-strain curves of compression test specimens.



Figure 17. Distorted compression test specimens.

Figure 18 shows the effect of zirconium dioxide and graphite weight percentage on the LM5/ZrO_2/Gr hybrid composites compressive strength. Zirconia has a monoclinic composition, while the composition of aluminum crystallizes in FCC. Their interface is due to the different crystalline structures of zirconia and aluminum that sounds incoherent [56]. This incoherence, therefore, increases the strength of the composite materials.

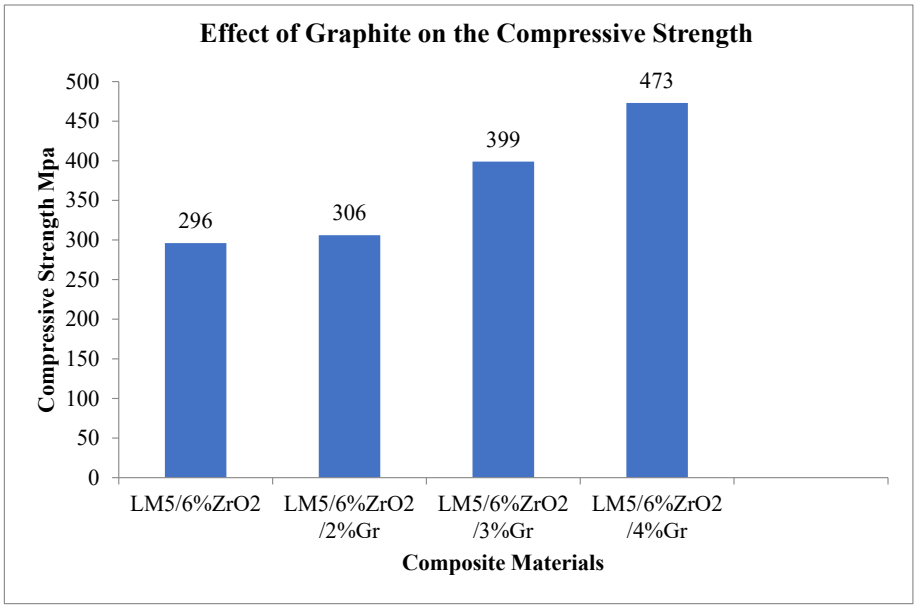


Figure 18. Effect of graphite on the compressive strength of composites.

The high hardness of the Al matrix composites is probably due to the high stiffness rate of the composites during their strain. Improvement of the hardening function may be related to the elastic properties of ZrO_2 particles, and their prevention of deformation of the matrix. Thus, in the presence of a suitable interface, the ZrO_2 particles prevent deformation of the matrix and increase work hardening. In addition, the specific thermal expansion coefficients of zirconia and aluminum produce stress that can boost the number of dislocations and, as a result, the strength of the composite. Increasing dislocation density and the piling up behind ZrO_2 particles serve as obstacles in the dislocation movement. The greater the sum of ZrO_2, the greater the number of dislocations that are formed. The compressive strength of the LM5/6% ZrO_2 alloy is 296 MPa. Results show that by adding the ZrO_2/Gr particles, the compressive strength of the aluminum alloy composite

is dramatically increased [57]. The compressive strength of the reinforced composite of aluminum alloy LM5 with 6% ZrO_2/2% Gr is 306 MPa, and this value increases to 399 MPa for LM5 with 6% ZrO_2/3% Gr, and further increases to 473 MPa for the composition of LM5/6% ZrO_2/4% Gr. From the experimental results, it is clear that the compressive strength of the hybrid composites are improved [58].

Figure 19 shows the effect of zirconia and graphite on the compression percentage. By adding 6% zirconium dioxide, the compressive percentage is 45.32%, loses its ductility, and the transition occurs from ductile to brittle. The compression of LM5 + 6% ZrO_2 + 2% graphite is 50.52%, this value is increased to 52.3% for the composition of LM5 + 6% of ZrO_2/3% graphite, and then increases again to 54.99% for the composition of LM5 + 6% of ZrO_2 + 4% graphite. The maximum compressive strength is observed at 6% ZrO_2/4% graphite.

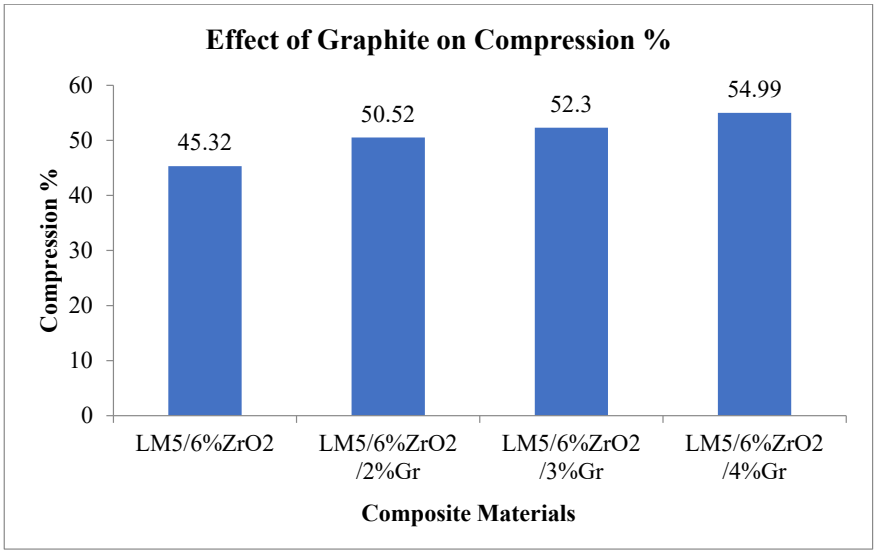


Figure 19. Effect of graphite on the compression of composites.

4.7. Impact Strength

The impact strength of the fabricated composites is determined by conducting an Izod impact test. Fractured impact test specimens are shown in Figure 20.

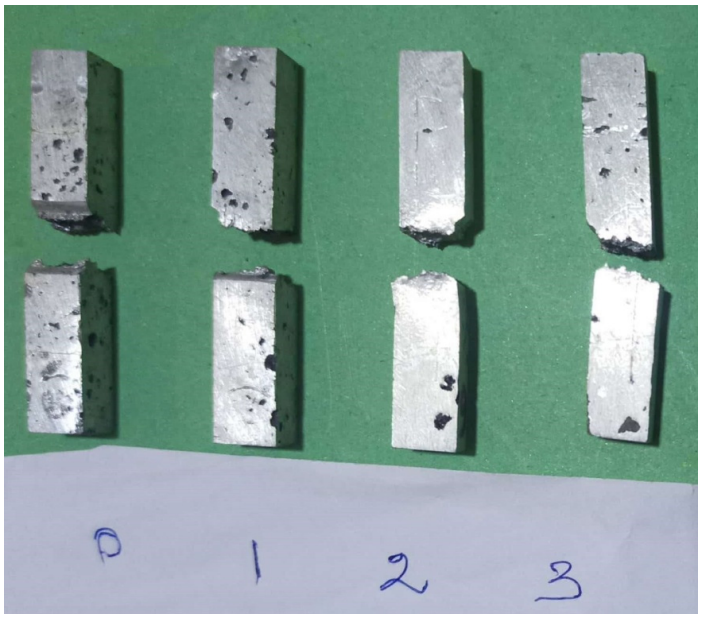


Figure 20. Fractured impact test specimens.

Figure 21 shows that the impact energy of the fabricated composites escalates with the increase in graphite percentage. The impact strength of LM5 reinforced with 6% Gr is 12 joules, and it is decreased to 9.15 joules in 6% ZrO_2/2% graphite, and then gradually increases to 9.25 and 9.35 in the 3% and 4% graphite composites, respectively. The impact energy increase with the strengthening could be due to the tough bond forming among the matrix and the reinforcing ZrO_2 and graphite. It is also noted that the impact strength of all the fabricated composites is relatively greater compared to the impact strength of the LM5 aluminum alloy (7.9 joules), due to the combined effect of zirconia and graphite [59].

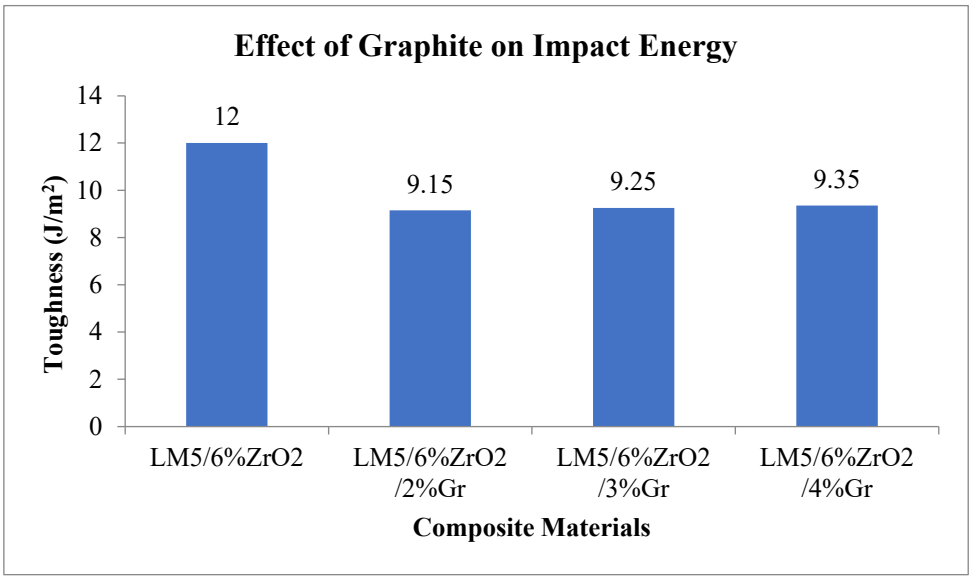


Figure 21. Effect of graphite on the toughness of composites.

5. Conclusions

This research examines the mechanical characterization and microstructural analysis of hybrid composites. The stir casting technique efficaciously fabricatesaluminum-based hybrid composites with an even distribution of ZrO_2 and graphite particles. Density is increased slightly, but micro- and macro-hardness are improved magnificently by increasing the fraction of weight of graphite in 6% ZrO_2. The impact, tensile, and compressive strength of MMCs are improved magnificently by increasing the fraction of weight of graphite in 6% ZrO_2. Elongation of the composites decreases due to the transformation of materials from ductile to brittle. An LM5 aluminum alloy reinforced with 6% ZrO_2/4% graphite can be used further for many structural applications, as it has improved mechanical properties such as compressive strength, hardness, and impact strength.

Author Contributions: Conceptualization, J.U.P. and S.J.J.; methodology, S.S.; formal analysis, S.J.J. and J.U.P.; investigation, H.M.A.H.; resources, S.J.J.; data curation, S.S. and S.R.G.; writing—original draft preparation, S.J.J.; writing—review and editing, J.U.P.; visualization, S.S. and S.R.G.; supervision, J.U.P.; project administration, S.S.; funding acquisition, H.M.A.H. All authors have read and agreed to the published version of the manuscript.

Funding: This research received no external funding.

Institutional Review Board Statement: Not applicable.

Informed Consent Statement: Not applicable.

Data Availability Statement: The data presented in this study are available through email upon request to the corresponding author.

Conflicts of Interest: The authors declare that they have no conflict of interest.

References

1. Surappa, M.K. Aluminium matrix composites: Challenges and Opportunities. *Sadhana* **2003**, *28*, 319–334. [CrossRef]
2. Srivatsan, T.S.; Ibrahim, I.A.; Mohamed, F.A.; Lavernia, E.J. Processing techniques for particulate-reinforced metal aluminum matrix composites. *J. Mater. Sci.* **1991**, *26*, 596–5978. [CrossRef]
3. Clyne, T.W.; Withers, P.J. *An Introduction to Metal Matrix Composites*; Cambridge University Press: Cambridge, UK, 1993.
4. Surappa, K.M.; Rohatgi, P.K. Preparation and properties of cast aluminum-ceramic particle composites. *J. Mater. Sci.* **1981**, *16*, 983–993. [CrossRef]
5. Lanker, M.V. *Metallurgy of Aluminum Alloys*; Chapman & Hall Ltd.: Boca Raton, FL, USA, 1967.
6. Hashim, J.; Looney, L.; Hashmi, M.S.J. Metal matrix composites: Production by the stir casting method. *J. Mater. Process. Technol.* **1999**, *92*, 1–7. [CrossRef]
7. Torralba, J.D.; Da Costa, C.E.; Velasco, F. P/M Aluminum matrix composites: An overview. *J. Mater. Process. Technol.* **2003**, *1–2*, 203–206. [CrossRef]
8. Pai, B.C.; Pillai, R.M.; Satyanarayana, K.G. Prospects for graphite aluminium composites in Engineering industries. *Ind. J. Eng. Mater. Sci.* **1994**, *1*, 279–285.
9. Syarifudin, M.; Hale, E.N.; Sofyan, B.T. Effect of ZrO_2 addition on mechanical properties and microstructure of Al-9Zn-6Mg-3Si matrix composites manufactured by squeeze casting. *Mater. Sci. Eng.* **2019**, *517*, 12001. [CrossRef]
10. James, S.J.; Annamalai, A.R. Machinability study of developed composite AA6061-ZrO_2 and analysis of influence of MQL. *Metals* **2018**, *8*, 472. [CrossRef]
11. Babu, L.G.; Ramesh, M.; Ravichandran, M. Mechanical and tribological characteristics of ZrO_2 reinforced Al2014 matrix composites produced via stir casting route. *Mater. Res. Express* **2019**, *6*, 115542.
12. Gunasekaran, T.; Vijayan, S.N.; Prakash, P.; Satishkumar, P. Mechanical properties and characterization of Al7075 aluminum alloy based ZrO_2 particle reinforced metal-matrix composites. *Mater. Today Proc.* **2020**, *in press*. [CrossRef]
13. Arif, M.; Asif, M.; Ahmed, I. Advanced composite material for aerospace application—A review. *Int. J. Eng. Manuf. Sci.* **2017**, *7*, 393–409.
14. Pandiyarajan, R.; Maran, P.; Murugan, N.; Marimuthu, S.; Sornakumar, T. Friction stir welding of hybrid AA 6061-ZrO_2-C composites FSW process optimization using desirability approach. *Mater. Res. Express* **2019**, *6*, 066553. [CrossRef]
15. Pul, M. Effect of ZrO_2 quantity on mechanical properties of ZrO_2-reinforced aluminum composites produced by the vacuum infiltration technique. *Rev. De Metal.* **2021**, *57*, e195. [CrossRef]
16. Moghanlou, F.S.; Nekahi, S.; Vajdi, M.; Ahmadi, Z.; Motallebzadeh, A.; Shokouhimehr, A.; Shokouhimehr, M.; Jafargholinejad, S.; Asl, M.S. Effects of graphite nano-flakes on thermal and microstructural properties of TiB2–SiC composites. *Ceram. Int.* **2020**, *46*, 11622–11630. [CrossRef]
17. Baradeswaran, A.; ElayaPerumal, A. Effect of graphite on tribological and mechanical properties of AA7075 composites. *Tribol. Trans.* **2015**, *58*, 1–6. [CrossRef]
18. Simsek, I.; Şimsek, D.; Ozyurek, D. The effect of different sliding speeds on wear behavior of ZrO_2 reinforcement aluminium matrix composite materials. *Int. Adv. Res. Eng. J.* **2020**, *4*, 1–7.
19. Rino, J.J.; Sivalingappa, D.; Koti, H.; Jebin, V.D. Properties of Al6063 MMC Reinforced with Zircon Sand and Alumina. *IOSR J. Mech. Civ. Eng.* **2013**, *5*, 72–77. [CrossRef]
20. HimaGireesh, C.; Durga Prasad, K.G.; Ramji, K. Experimental investigation on mechanical properties of an Al6061 hybrid metal matrix composite. *J. Compos. Sci.* **2018**, *2*, 49. [CrossRef]
21. Aruna, K.; Diwakar, K.; Kumar, K.B. Development and Characterization of Al 6061-ZrO_2 Reinforced Metal Matrix Composites. *Int. J. Adv. Res. Comput. Sci. Softw. Eng.* **2018**, *8*, 270–275.
22. Kareem, A.; Qudeiri, J.A.; Abdudeen, A.; Ahammed, T.; Ziout, A. A review on AA 6061 metal matrix composites produced by stir casting. *Materials* **2021**, *14*, 175. [CrossRef]
23. Karthikeyan, G.; Jinu, G.R. Dry sliding wear behaviour of stir cast LM25/ZrO_2 metal matrix composites. *Trans. FAMENA* **2015**, *39*, 89–98.
24. JebaroseJuliyana, S.; UdayaPrakash, J. Drilling parameter optimization of metal matrix composites (LM5/ZrO_2) using Taguchi Technique. *Mater. Today Proc.* **2020**, *33*, 3046–3050. [CrossRef]
25. Madhusudhan, M.; Naveen, G.J.; Mahesha, K. Mechanical characterization of AA7068- ZrO_2 reinforced metal matrix composites. *Mater. Today Proc.* **2017**, *4*, 3122–3130. [CrossRef]
26. Sozhamannan, G.G.; BalasivanandhaPrabu, S.; Venkatajalapathy, V.S.K. Effect of processing parameters on metal matrix composites: Stir casting process. *J. Surf. Eng. Mater. Adv. Technol.* **2012**, *2*, 11–15.
27. Malaki, M.; FadaeiTehrani, A.; Niroumand, B.; Gupta, M. Wettability in metal matrix composites. *Metals* **2021**, *11*, 1034. [CrossRef]
28. Liao, Z.; Standke, Y.; Gluch, J.; Balázsi, K.; Pathak, O.; Höhn, S.; Herrmann, M.; Werner, S.; Dusza, J.; Balázsi, C.; et al. Microstructure and fracture mechanism investigation of porous silicon Nitride–Zirconia–Graphene composite using multi-Scale and In-Situ microscopy. *Nanomaterials* **2021**, *11*, 285. [CrossRef] [PubMed]
29. Alajmi, M.; Shalwan, A. Correlation between mechanical properties with specific wear rate and the coefficient of friction of graphite/epoxy composites. *Materials* **2015**, *8*, 4162–4175. [CrossRef]
30. Molina, J.M.; Rodríguez-Guerrero, A.; Louis, E.; Rodríguez-Reinoso, F.; Narciso, J. Porosity effect on thermal properties of Al-12 wt% Si/graphite composites. *Materials* **2017**, *10*, 177. [CrossRef] [PubMed]

31. Smeulders, R.J.; Mischgofsky, F.H.; Frankena, H.J. Direct microscopy of alloy nucleation, solidification and ageing (coarsening) during stir casting. *J. Cryst. Growth* **1986**, *76*, 151–169. [CrossRef]
32. Zhou, W.; Xu, Z.M. Casting of SiC reinforced metal matrix composites. *J. Mater. Process. Technol.* **1997**, *63*, 358–363. [CrossRef]
33. Callister, W.D., Jr. *Material Science and Engineering—An Introduction*, 2nd ed.; John Wiley: New York, NY, USA, 1991.
34. Ravi, B.; BaluNaik, B.; UdayaPrakash, J. Characterization of Aluminum Matrix Composites (AA6061/B4C) Fabricated by Stir Casting Technique. *Mater. Today Proc.* **2015**, *2*, 2984–2990. [CrossRef]
35. Lindroos, V.K.; Talvitie, M.J. Recent advances in metal matrix composites. *J. Mater. Process. Technol.* **1995**, *53*, 273–284. [CrossRef]
36. Razzaq, A.M.; Majid, D.L.; Basheer, U.M.; Aljibori, H.S.S. Research Summary on the Processing, Mechanical and Tribological Properties of Aluminium Matrix Composites as Effected by Fly Ash Reinforcement. *Crystals* **2021**, *11*, 1212. [CrossRef]
37. Chan, K.F.; Zaid, M.H.M.; Mamat, M.S.; Liza, S.; Tanemura, M.; Yaakob, Y. Recent developments in carbon nanotubes-reinforced ceramic matrix composites: A review on dispersion and densification techniques. *Crystals* **2021**, *11*, 457. [CrossRef]
38. Lokesh, T.; Mallikarjun, U.S. Mechanical and morphological studies of Al6061-Gr-SiC hybrid metal matrix composites. *Appl. Mech. Mater.* **2015**, *813*, 195–202. [CrossRef]
39. Gowrishankar, T.P.; Manjunatha, L.H.; Sangmesh, B. Mechanical and Wear behaviour of Al6061 reinforced with Graphite and TiC Hybrid MMC's. *Mater. Res. Innov.* **2019**, *24*, 179–185.
40. Girisha, K.B.; Chittappa, H.C. Preparation, Characterization and Wear Study of Aluminum Alloy (Al 356.1) Reinforced with Zirconium Nano Particles. *Int. J. Innov. Res. Sci. Eng. Technol.* **2013**, *2*, 3627–3637.
41. Malhotra, S.; Narayan, R.; Gupta, R.D. Synthesis and Characterization of Aluminum 6061 Alloy-Fly ash& Zirconia Metal Matrix Composite. *Int. J. Curr. Eng. Technol.* **2013**, *3*, 1716–1719.
42. Baghchesara, M.A.; Abdizadeh, H.; Baharvandi, H.R. Microstructure and Mechanical Poperties of Aluminum Alloy Matrix Composite Reinforced with ZrO_2 Particles. *Asian J. Chem.* **2010**, *22*, 3824–3834.
43. Yadav, P.; Ranjan, A.; Kumar, H.; Mishra, A.; Yoon, J. A contemporary review of aluminium MMC developed through stir-casting route. *Materials* **2021**, *14*, 6386. [CrossRef]
44. Barabás, R.; Fort, C.I.; Turdean, G.L.; Bizo, L. Influence of HAP on the morpho-structural properties and corrosion resistance of ZrO_2-based composites for biomedical applications. *Crystals* **2021**, *11*, 202. [CrossRef]
45. Nakonieczny, D.S.; Slíva, A.; Paszenda, Z.; Hundáková, M.; Kratošová, G.; Holešová, S.; Majewska, J.; Kałużyński, P.; Sathish, S.K.; SimhaMartynková, G. Simple approach to medical grade alumina and zirconia ceramics surface alteration via acid etching treatment. *Crystals* **2021**, *11*, 1232. [CrossRef]
46. Liu, J.; Sun, K.; Zeng, L.; Wang, J.; Xiao, X.; Liu, J.; Guo, C.; Ding, Y. Microstructure and Properties of Copper–Graphite Composites Fabricated by Spark Plasma Sintering Based on Two-Step Mixing. *Metals* **2020**, *10*, 1506.
47. Malaki, M.; Xu, W.; Kasar, A.K.; Menezes, P.L.; Dieringa, H.; Varma, R.S.; Gupta, M. Advanced metal matrix nanocomposites. *Metals* **2019**, *9*, 330. [CrossRef]
48. Singh, M.; Garg, H.K.; Maharana, S.; Yadav, A.; Singh, R.; Maharana, P.; Nguyen, T.V.; Yadav, S.; Loganathan, M.K. An experimental investigation on the material removal rate and surface roughness of a hybrid aluminum metal matrix composite (Al6061/sic/gr). *Metals* **2021**, *11*, 1449. [CrossRef]
49. Khan, A.; Abdelrazeq, M.W.; Mattli, M.R.; Yusuf, M.M.; Alashraf, A.; Matli, P.R.; Shakoor, R.A. Structural and mechanical properties of Al-SiC-ZrO_2 nanocomposites fabricated by microwave sintering technique. *Crystals* **2020**, *10*, 904. [CrossRef]
50. Díaz, M.; Smirnov, A.; Gutiérrez-González, C.F.; Estrada, D.; Bartolomé, J.F. Microstructure and mechanical properties of zirconia (3Y-TZP)/Zr composites prepared by wet processing and subsequent spark plasma sintering. *Ceramics* **2020**, *3*, 53–64. [CrossRef]
51. Kvashnin, V.I.; Dudina, D.V.; Ukhina, A.V.; Koga, G.Y.; Georgarakis, K. The Benefit of the Glassy State of Reinforcing Particles for the Densification of Aluminum Matrix Composites. *J. Compos. Sci.* **2022**, *6*, 135. [CrossRef]
52. Simoncini, A.; Tagliaferri, V.; Ucciardello, N. High thermal conductivity of copper matrix composite coatings with highly-aligned graphite nanoplatelets. *Materials* **2017**, *10*, 1226. [CrossRef]
53. Sadhana, A.D.; Prakash, J.U.; Sivaprakasam, P.; Ananth, S. Wear behaviour of aluminum matrix composites (LM25/Fly Ash)-A Taguchi approach. *Mater. Today Proc.* **2020**, *33*, 3093–3096. [CrossRef]
54. Prakash, J.U.; Juliyana, S.J.; Pallavi, P.; Moorthy, T.V. Optimization of Wire EDM Process Parameters for Machining Hybrid Composites (356/B4C/Fly Ash) using Taguchi Technique. *Mater. Today Proc.* **2018**, *5*, 7275–7283.
55. Rubi, C.S.; Prakash, J.U. Drilling of Hybrid Aluminum Matrix Composites using Grey-Taguchi Method. *INCAS Bull.* **2020**, *12*, 167–174.
56. Seon, G.; Makeev, A.; Schaefer, J.D.; Justusson, B. Measurement of interlaminar tensile strength and elastic properties of composites using open-hole compression testing and digital image correlation. *Appl. Sci.* **2019**, *9*, 2647.
57. Deng, C.; Li, R.; Yuan, T.; Niu, P.; Wang, Y. Microstructure and Mechanical Properties of a Combination Interface between Direct Energy Deposition and Selective Laser Melted Al-Mg-Sc-Zr Alloy. *Metals* **2021**, *11*, 801.
58. Chandel, R.; Sharma, N.; Bansal, S.A. A review on recent developments of aluminum-based hybrid composites for automotive applications. *Emergent Mater.* **2021**, *4*, 1243–1257.
59. Jadhav, P.R.; Sridhar, B.R.; Nagaral, M.; Harti, J.I. Mechanical behavior and fractography of graphite and boron carbide particulates reinforced A356 alloy hybrid metal matrix composites. *Adv. Compos. Hybrid Mater.* **2020**, *3*, 114–119.